LETTER

doi:10.1038/nature11259

Bacterial virulence proteins as tools to rewire kinase pathways in yeast and immune cells

Ping Wei[1,2]*, Wilson W. Wong[1,2,3]*†, Jason S. Park[1,2,3], Ethan E. Corcoran[2,3,4]†, Sergio G. Peisajovich[1,2]†, James J. Onuffer[1,3], Arthur Weiss[2,3,4] & Wendell A. Lim[1,2,3]

Bacterial pathogens have evolved specific effector proteins that, by interfacing with host kinase signalling pathways, provide a mechanism to evade immune responses during infection[1,2]. Although these effectors contribute to pathogen virulence, we realized that they might also serve as valuable synthetic biology reagents for engineering cellular behaviour. Here we exploit two effector proteins, the *Shigella flexneri* OspF protein[3] and *Yersinia pestis* YopH protein[4], to rewire kinase-mediated responses systematically both in yeast and mammalian immune cells. Bacterial effector proteins can be directed to inhibit specific mitogen-activated protein kinase pathways selectively in yeast by artificially targeting them to pathway-specific complexes. Moreover, we show that unique properties of the effectors generate new pathway behaviours: OspF, which irreversibly inactivates mitogen-activated protein kinases[4], was used to construct a synthetic feedback circuit that shows novel frequency-dependent input filtering. Finally, we show that effectors can be used in T cells, either as feedback modulators to tune the T-cell response amplitude precisely, or as an inducible pause switch that can temporarily disable T-cell activation. These studies demonstrate how pathogens could provide a rich toolkit of parts to engineer cells for therapeutic or biotechnological applications.

Many bacterial pathogens have developed an array of effector proteins to rewire host signalling networks and downregulate the immune response[2] (Fig. 1a). Some effectors mimic host activities, such as the *Y. pestis* effector YopH, which is a highly active phosphotyrosine phosphatase[3]. Other effectors use unusual mechanisms, such as the *S. flexneri* OspF protein, which irreversibly inactivates mitogen-activated protein kinases (MAPKs) by catalysing a β-elimination reaction that removes the hydroxyl group of the key phosphothreonine side chain[4].

MAPK pathways have a central role in diverse eukaryotic responses, ranging from immune response to cell-fate decisions[5,6]. Thus, the ability to tune MAPK response would facilitate engineering cells for diverse therapeutic and biotechnological applications[7,8]. Recent work has shown that MAPK signalling dynamics in yeast can be reshaped with synthetic feedback loops that involve controlled expression and targeting of pathway modulators to appropriate signalling complexes[9]. Identifying effective pathway modulators is challenging; thus we considered that pathogen effector proteins may have untapped use as components for predictably and systematically engineering signalling pathways. Here we use the effector proteins OspF and YopH to modulate kinase signalling pathways in yeast and in human primary T cells.

We first introduced OspF into yeast. As reported[10], overexpression of OspF led to growth inhibition under standard conditions, hyperosmotic stress conditions (Fig. 1b) and cell-wall-damaging conditions (Supplementary Fig. 1a). OspF contains a canonical docking peptide at its amino (N) terminus that allows it to bind several MAPKs in yeast[11]. We found that expression of an OspF mutant lacking its native docking peptide (ΔN-OspF) yielded normal growth behaviour under all conditions (Fig. 1b and Supplementary Fig. 1a). Next we tested whether ΔN-OspF could be redirected to a specific pathway by tagging the protein with a leucine zipper heterodimerization motif, and fusing the complementary interacting motif to Pbs2, the scaffold protein that organizes the osmolarity MAPK pathway. This targeted version of ΔN-OspF only showed a growth defect under high salt conditions, showing that OspF activity could be engineered to inhibit a specific MAPK (Fig. 1b).

To explore re-targeting OspF to specific pathways further, we engineered yeast strains in which ΔN-OspF was selectively targeted to either the osmolarity MAPK complex or the mating MAPK complex (by targeting it to the mating pathway scaffold protein, Ste5) (Fig. 1c). Targeting of ΔN-OspF to the Pbs2 inhibited the osmolarity response but not the mating response. Conversely, when ΔN-OspF was targeted to Ste5, only the mating response was inhibited. Thus, the inhibitory activity of this effector could be selectively aimed at one of several MAPK pathways in the same cell.

One of the unique aspects of OspF is that it catalyses an irreversible inactivation of MAPKs (unlike reversible dephosphorylation by a phosphatase). Thus MAPK activity can only be restored through new protein synthesis, which has a much slower timescale than re-phosphorylation (Fig. 2a, b). This longer timescale would be expected to lead to an extended refractory period after OspF action, during which the targeted MAPK pathway could no longer respond to subsequent stimuli.

Computational simulations indicated that a long refractory period could result in significant changes to the frequency-dependent behaviour of pathway response (Supplementary Fig. 2). There is growing evidence that cells use frequency modulation of diverse molecular events to encode and transmit information[12,13]. Our models indicated that with a negative feedback loop (that is, MAPK activity induced expression of OspF), pathway output would be dampened when input periods are long enough to accumulate significant amounts of the negative effector but shorter than the refractory period (Supplementary Fig. 2).

To test if OspF could be used to filter frequency dependent inputs, we constructed a synthetic negative feedback loop in the yeast osmo-response pathway by expressing OspF targeted to the osmo-response signalling complex (ΔN-OspF–zipper) from the Hog1 responsive promoter, *pSTL1* (Fig. 2c). As a comparison, we also engineered an analogous synthetic feedback loop using a reversible Hog1 MAPK inhibitory protein—the yeast MAPK phosphatase, PTP2. Phospho-Hog1 translocation to the nucleus was used as a fast-timescale output reporter (Supplementary Fig. 3)[14–16]. To measure integrated output over a longer timescale, we also measured a slower timescale

[1]Department of Cellular and Molecular Pharmacology, University of California San Francisco, San Francisco, California 94158, USA. [2]Howard Hughes Medical Institute, University of California San Francisco, San Francisco, California 94158, USA. [3]The Cell Propulsion Laboratory, University of California San Francisco, San Francisco, California 94158, USA. [4]Department of Medicine, University of California San Francisco, San Francisco, California 94158, USA. †Present addresses: Department of Biomedical Engineering, Boston University, Boston, Massachusetts 02215, USA (W.W.W.); Department of Pulmonology and Critical Care Medicine, Northwest Permanente P.C., 10180 SE Sunnyside Road, Clackamas, Oregon 97015, USA (E.E.C.); Department of Cell & Systems Biology, University of Toronto, Toronto, Ontario M5S 3G5, Canada (S.G.P.).
*These authors contributed equally to this work.

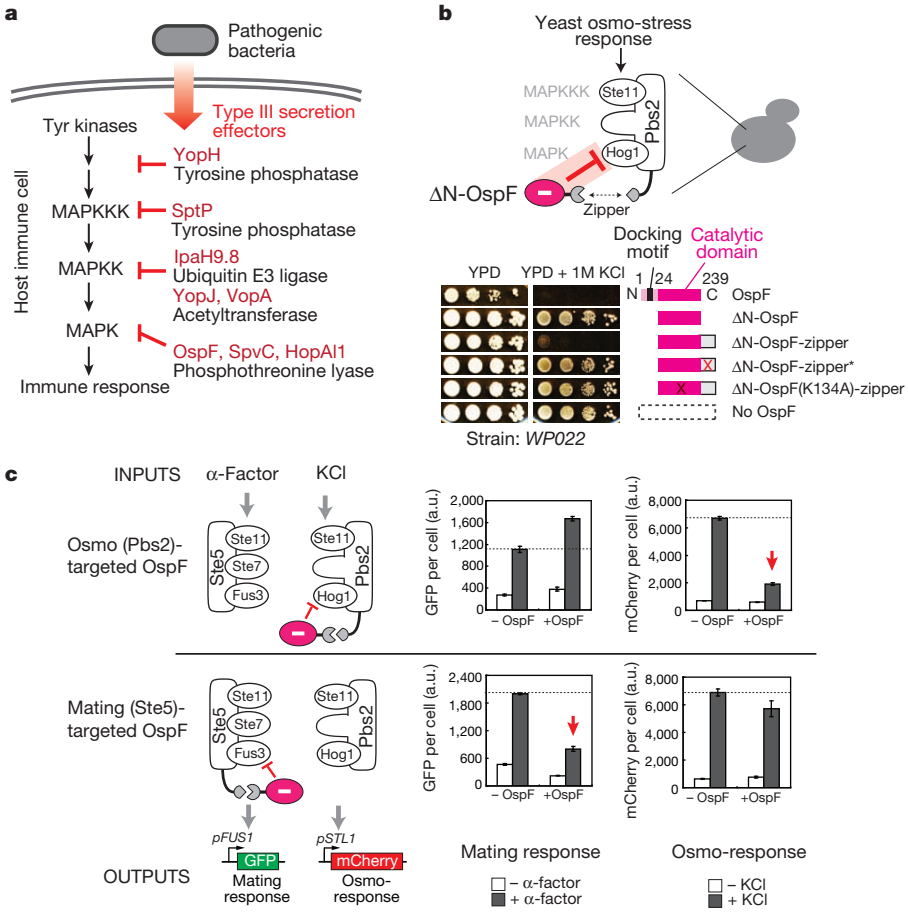

Figure 1 | Bacterial effector OspF can block selective MAPK pathways in yeast. **a**, Type III secretion effectors that modulate host kinase signalling. MAPKKK, MAP-kinase kinase kinase. **b**, Targeting of OspF to yeast osmolarity pathway. Wild-type OspF impairs growth on rich media, but is rescued by docking motif deletion (ΔN-OspF). Recruitment of ΔN-OspF to osmolarity scaffold Pbs2 by leucine zipper selectively blocks growth on 1 M KCl (zipper*, mutant leucine zipper; K134A, catalytic dead mutant of OspF). **c**, ΔN-OspF selectively inhibits mating or osmolarity if targeted to appropriate scaffold complex, assayed using pathway-specific transcriptional reporters. Average fluorescence and s.d. of three experiments are shown. a.u., arbitrary units.

transcriptional reporter—expression of mCherry from the *pSTL1* promoter.

We found that the OspF-mediated negative feedback circuit altered the osmo-stress pathway response to intermediate frequency stimulation, but not to continuous stress or to high-frequency stimulation (Fig. 2d and Supplementary Fig. 4a). Furthermore, in the course of stimulating cells with pulses of KCl of varying length, we discovered that an input period of approximately 16 min (intermediate frequency) leads to highly divergent transcriptional responses (Fig. 2d). Examination of Hog1 nuclear import in the OspF feedback strain shows that after three pulses, the amount of Hog1 competent for nuclear localization has decreased to near zero, consistent with a model in which—in this timeframe—there is sufficient OspF to inactivate the bulk of the Hog1 population and now to render the cells refractory to further pulses of stimulation. The cells containing a PTP2 negative feedback circuit do not show this marked filtering at this frequency. With higher frequency stimulation (2 min period), the three strains also do not significantly differ from each other in response, presumably because there is inadequate activation time with each pulse to build up a sufficient concentration of effector[17].

A broad frequency dependence analysis shows that the wild-type osmo-response pathway functions as a band-pass filter, with maximal response at intermediate frequencies, whereas the engineered pathway more closely resembles a low-pass filter, with maximal responses at low frequency (Fig. 2e). These distinct frequency filtering behaviours fit those predicted by computational simulations (Supplementary Fig. 2d).

We then sought to test whether these bacterial effectors could be used to rewire signalling in immune cells. Human T cells are an attractive synthetic biology platform because they can be isolated from patients, genetically engineered *ex vivo* and then transferred back into patients to treat cancer and chronic infection[18,19]. Although promising, the therapeutic application of engineered T cells carries risks of adverse side effects including inadvertent autoimmune-like attack of off-target host tissues[20,21]. Thus mechanisms to control the specificity, amplitude and timing of T-cell function are critical to balance therapeutic action against off-target toxicity.

Both OspF and YopH can modify the T-cell receptor (TCR) pathway (Fig. 3a). OspF inactivates the MAPK extracellular signal-regulated kinase (ERK), which is a central component of TCR signalling[4,22], whereas YopH dephosphorylates phospho-tyrosine, including the T-cell scaffold proteins LAT and SLP-76 (ref. 23). Constitutive expression of YopH and OspF in *Jurkat* T cells leads to severe inhibition of TCR activation, as measured by an NFAT transcriptional reporter[24] (Fig. 3a) (as well as other reporters of T-cell activation; Supplementary Fig. 5a). Expression of the catalytic dead versions of YopH and OspF had no effect on the TCR activation (Supplementary Fig. 5b). In addition, we showed that these two effectors clearly target distinct steps of the T-cell activation pathway, because induction of the T cells with the combination of phorbol 12-myristate 13-acetate (PMA) and ionomycin, which activates the T cell downstream of the PLCγ1-LAT/SLP76 dependent response, bypassed YopH inhibition[25], but was sensitive to OspF inhibition (Fig. 3a and Supplementary Fig. 5a). Thus, distinct pathogen effector proteins can be used to block this

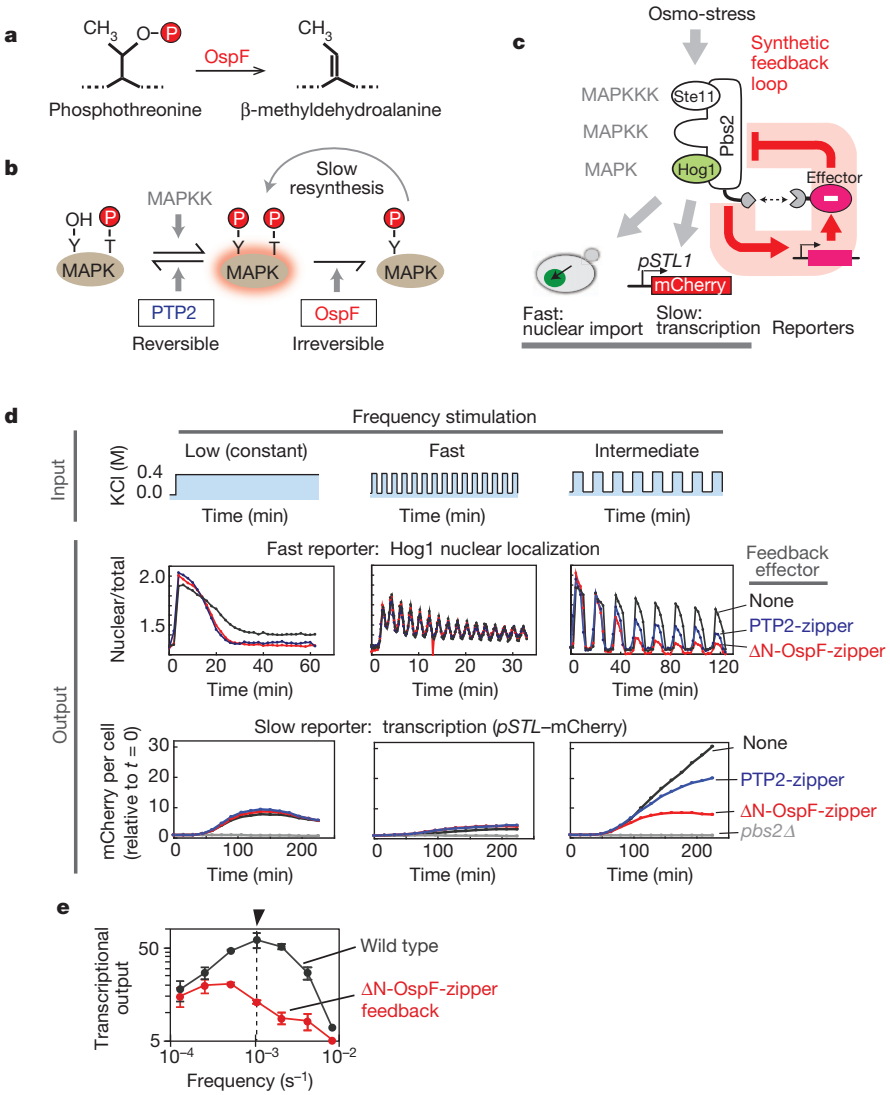

Figure 2 | Tuning-frequency-dependent response of yeast osmolarity pathway using synthetic OspF feedback loop. **a**, OspF is MAPK phosphothreonine lyase. **b**, OspF irreversibly inhibits MAPK activity. **c**, Synthetic negative feedback loop was built by expressing OspF from osmo-inducible *pSTL1* promoter. Hog1–GFP nuclear accumulation (Nuc:Tot ratio) was measured as a fast output reporter. *pSTL1*–mCherry served as a slower, gene expression reporter. **d**, Cells were stimulated with variable frequency inputs: low (constant), high (period = 2 min) and intermediate (period = 16 min). Significant difference in response to intermediate frequency stimulation is observed. **e**, Frequency–response curves for wild-type and OspF feedback strains (arrow: period = 16 min). Each point is average of 50–100 cells; s.d. from three repeats is shown. More detail on the frequency analysis is given in Supplementary Figs 2–4.

pathway at particular steps, much like a specific small-molecule inhibitor.

Given the ability of OspF and YopH to modulate T-cell responses, we sought to use these proteins to build circuits that could, in principle, improve the safety of therapeutic T cells. In adoptive T-cell therapy, a challenge is to limit over-activation or off-target activation of T cells that could lead to killing of host cells or to cytokine storm—a life-threatening immune response. One approach is to incorporate a safety 'kill switch'[26–28] into the T cells, such as the herpes simplex virus thymidine kinase gene. This protein converts the pro-drug ganciclovir into an inhibitor of replication, thus killing cells expressing the gene. Although herpes simplex virus thymidine kinase is currently being tested in a phase III clinical trial for the treatment of graft versus host disease in bone marrow transplants, this strategy irreversibly destroys the engineered, adoptively transferred cells[29]. Thus, instead of killing the engineered cells, we sought to design circuits that would limit the amplitude of the T-cell response or to pause T-cell activity temporarily.

We first tested whether bacterial effectors could be used to limit the response amplitude of *Jurkat* T cells. Negative feedback loops can act to limit the maximal amplitude of a response[30], so we engineered a library of negative feedback loops in which the OspF and YopH were expressed from a series of TCR-responsive promoters of varying strength (AP1 and NFAT) (Fig. 3b and Supplementary Fig. 7). For further tuning of feedback parameters, we also tagged effectors with degradation sequences (PEST motif) that reduce the half-life of the effectors. This series of negative feedback loops led to controlled reduction of the maximal response amplitude of T-cell activation (Fig. 3b). Moreover, the amplitude could be tuned systematically by varying feedback promoter strength and effector stability (Supplementary Fig. 7b). For example, expression of OspF from the strong feedback (*pNFAT*) promoter leads to a very low maximal response amplitude, but this effect could be systematically tuned by destabilizing the OspF effector with a PEST tag.

We also tested whether the bacterial effectors could be used to construct pause switches, which could transiently and reversibly disable T cells. We placed the effectors under the control of a tetracycline inducible promoter (*pTRE*), which allowed external control of the timing of effector expression with the addition of doxycycline.

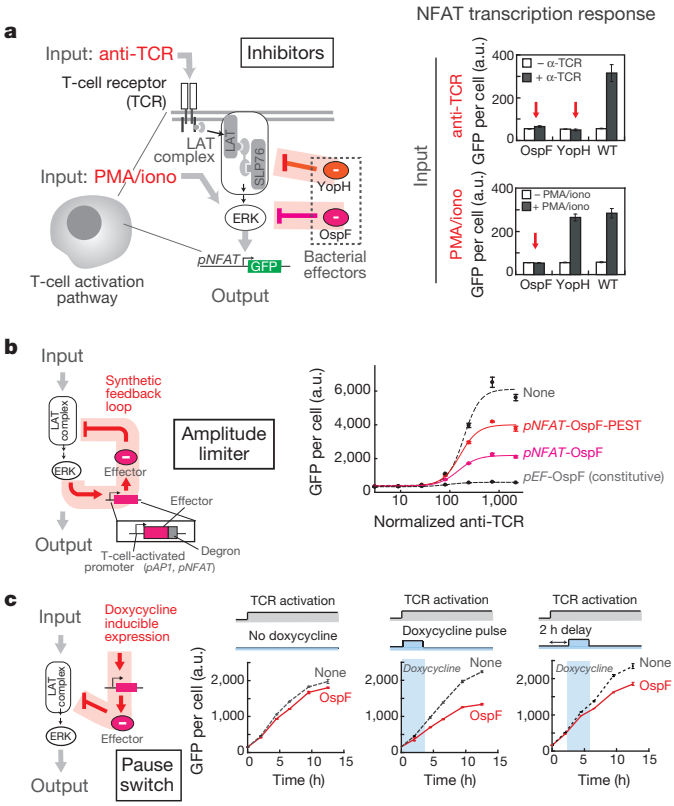

Figure 3 | OspF can be used to control T-cell activation amplitude and duration precisely in *Jurkat* T cells. **a**, Constitutively expressed OspF and YopH inhibit specific steps in the TCR pathway. Activation of NFAT transcription by anti-TCR antibody versus PMA/ionomycin is shown. **b**, Synthetic amplitude limiters were constructed using negative feedback loops with different effectors, promoters and degrons. Dose–response curves of the *pNFAT*-OspF circuit, with or without degron, are shown. **c**, Synthetic pause switch was built by expressing OspF from a doxycycline-inducible promoter, *pTRE*. A 4 h pulse induction disabled T-cell response when initiated at 0 or 2 h after T-cell stimulation. Standard deviation from three samples is shown.

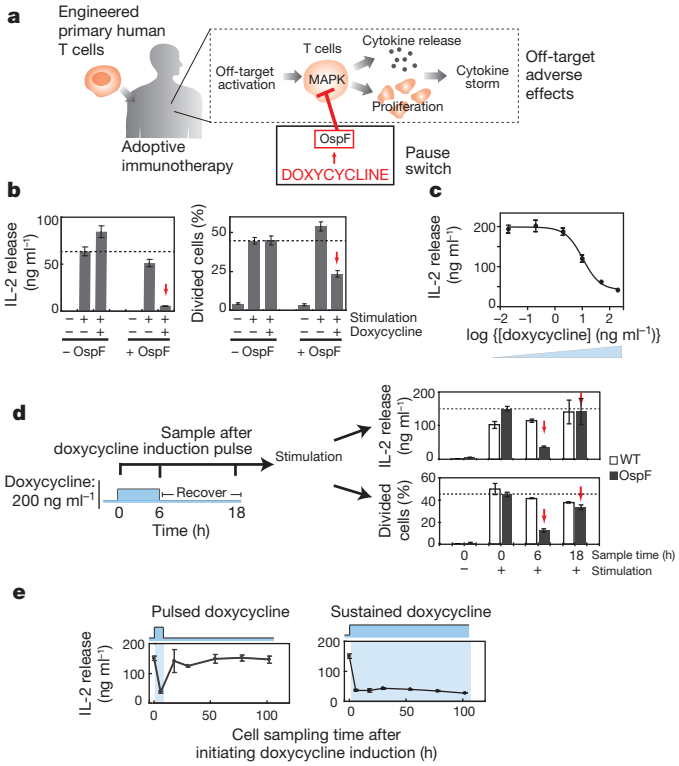

Figure 4 | OspF can be used as a synthetic pause switch to control human primary CD4$^+$ T-cell activation. **a**, Off-target activation of transplanted T cells can induce cytokine storm in adoptive immunotherapy. A pause switch could prevent this adverse response. **b**, Six-hour pre-induction of OspF by doxycycline inhibited IL-2 release and proliferation of activated CD4$^+$ T cells. **c**, Six-hour pre-treatment with different doses of doxycycline can tune IL-2 release. **d**, Cells treated with 6 h doxycycline pulse were sampled at different times after the pulse, then subjected to a 24 h IL-2 release assay or a 4 day proliferation assay. **e**, IL-2 release can be inhibited either transiently or in a sustained manner by varying the duration of doxycycline treatment. Average and s.d. of three experimental repeats are shown.

Effectors were fused to a destabilization domain so that they would be rapidly degraded once doxycycline is removed. Using this system, we first showed that transient expression of bacterial effectors can inhibit TCR signalling after the pathway is activated in *Jurkat* T cells (Fig. 3c). TCR signalling can be inhibited up to 6 h after activation using this approach (Supplementary Fig. 8b). Finally, we showed that engineered T cells can be subjected to cycles of TCR activation, paused with a short period of induced expression of the bacterial effector, and then reactivated after this pause (Supplementary Fig. 8c).

We then tested the pause switch in a clinically important cell type for adoptive immunotherapy—primary human CD4$^+$ T cells (in contrast to the *Jurkat* T-cell line, which does not require cytokine or TCR activation to stimulate proliferation). We showed that when OspF is induced by the addition of doxycycline, both interleukin-2 (IL-2) release and cell proliferation were inhibited in a dose-dependent manner (Fig. 4b, c). Activation of the TCR by anti-CD3/CD28 and antigen-presenting cells can also be inhibited by expression of OspF (Supplementary Fig. 9a). Moreover, after doxycycline is removed, IL-2 release and cell division recovers in 6–18 h (Fig. 4d, e). Sustained exposure to doxycycline can inhibit T-cell activity over the course of several days (Fig. 4e) without having any significant effect on cell viability (Supplementary Fig. 9c). Thus this work provides a proof of principle for the design of a simple 'pause' switch that could allow external control over the timing and level of T-cell activation and cytokine release, to minimize adverse events associated with adoptive immunotherapy such as cytokine storm.

Most work on bacterial pathogen effector proteins has the long-term aim of neutralizing the pathogens' infectious capabilities. We have shown, however, that bacterial effectors can also be valuable synthetic biology tools, because of their unique biochemical properties. We have used bacterial effectors to modulate MAPK signalling in yeast to generate novel time-dependent dynamics. We have also shown that bacterial effectors can be used to tune human TCR signalling dynamics flexibly, with potential application as safety switches for adoptive immunotherapy. The vast array of bacterial pathogen effector proteins, beyond those studied here, holds promise as a rich and important source of parts for the cellular engineering toolkit.

METHODS SUMMARY

Flow cytometry experiments. Analysis of the pathway-dependent fluorescent protein (green fluorescent protein (GFP) and mCherry) expression in yeast cells and phosphorylated ERK in *Jurkat* T cells was performed with a BD LSRII flow cytometer (BD Biosciences) equipped with a high-throughput sampler. α-Factor (1.5 μM; GenScript) or 0.4 M of KCl were added into yeast cultures to induce separately the mating- or osmo-specific pathway response. For staining of phosphorylated ERK in *Jurkat* T cells, cells were fixed, made permeable by incubation with ice-cold 90% methanol on ice for 30 min and stained with primary antibody to phosphorylated ERK (Cell Signaling) and anti-rabbit APC secondary antibody (Jackson Immunoresearch).

Microfluidics and fluorescent microscopy. Microfluidic yeast cell culture was performed in Y04C plates with an ONIX flow control system (Cellasic). Cells were loaded into the flow chamber pre-coated with concanavalin A. Pulse stimulation with salt media was performed by ONIX FG flow control software (Cellasic) with a flow pressure of 8 pounds per square inch. Image acquisition was performed with a TE2000-E automated inverted microscope (Nikon) with Perfect Focus and a ×100

oil immersion lens. Image analysis for both nuclear Hog1–GFP import and *pSTL1*–mCherry expression was performed with custom MATLAB (Mathworks) software.

Human T-cell activation assay. Resting human primary $CD4^+$ cells (transduced with the pause switch constructs or untransduced) were pretreated with 200 ng ml^{-1} doxycycline for 6 h. Fifty thousand cells were placed in a 96-well plate with 200 µl human growth media with activation agents added (10 ng ml^{-1} PMA + 0.5 µM ionomycin, magnetic Dynabeads coated with anti-CD3/anti-CD28 (beads:cells ratio, 0.3:1)). After 24 h of incubation at 37 °C, the released IL-2 in the supernatant was measured with a human IL-2 ELISA kit II (BD Biosciences). Cells labelled with CellTrace Violet dye (Invitrogen) were assayed by flow cytometry after incubation for 4 days to quantify cell proliferation.

Full Methods and any associated references are available in the online version of the paper.

Received 21 March; accepted 25 May 2012.
Published online 22 July 2012.

1. Ribet, D. & Cossart, P. Pathogen-mediated posttranslational modifications: a re-emerging field. *Cell* **143,** 694–702 (2010).
2. Broberg, C. A. & Orth, K. Tipping the balance by manipulating post-translational modifications. *Curr. Opin. Microbiol.* **13,** 34–40 (2010).
3. Zhang, Z. Y. *et al.* Expression, purification, and physicochemical characterization of a recombinant *Yersinia* protein tyrosine phosphatase. *J. Biol. Chem.* **267,** 23759–23766 (1992).
4. Li, H. *et al.* The phosphothreonine lyase activity of a bacterial type III effector family. *Science* **315,** 1000–1003 (2007).
5. Shaw, A. S. & Filbert, E. L. Scaffold proteins and immune-cell signalling. *Nature Rev. Immunol.* **9,** 47–56 (2009).
6. Dong, C., Davis, R. J. & Flavell, R. A. MAP kinases in the immune response. *Annu. Rev. Immunol.* **20,** 55–72 (2002).
7. Khalil, A. S. & Collins, J. J. Synthetic biology: applications come of age. *Nature Rev. Genet.* **11,** 367–379 (2010).
8. Purnick, P. E. & Weiss, R. The second wave of synthetic biology: from modules to systems. *Nature Rev. Mol. Cell Biol.* **10,** 410–422 (2009).
9. Bashor, C. J., Helman, N. C., Yan, S. & Lim, W. A. Using engineered scaffold interactions to reshape MAP kinase pathway signaling dynamics. *Science* **319,** 1539–1543 (2008).
10. Kramer, R. W. *et al.* Yeast functional genomic screens lead to identification of a role for a bacterial effector in innate immunity regulation. *PLoS Pathog.* **3,** e21 (2007).
11. Zhu, Y. *et al.* Structural insights into the enzymatic mechanism of the pathogenic MAPK phosphothreonine lyase. *Mol. Cell* **28,** 899–913 (2007).
12. Nelson, D. E. *et al.* Oscillations in NF-κB signaling control the dynamics of gene expression. *Science* **306,** 704–708 (2004).
13. Cai, L., Dalal, C. K. & Elowitz, M. B. Frequency-modulated nuclear localization bursts coordinate gene regulation. *Nature* **455,** 485–490 (2008).
14. Muzzey, D., Gomez-Uribe, C. A., Mettetal, J. T. & van Oudenaarden, A. A systems-level analysis of perfect adaptation in yeast osmoregulation. *Cell* **138,** 160–171 (2009).
15. Mettetal, J. T., Muzzey, D., Gomez-Uribe, C. & van Oudenaarden, A. The frequency dependence of osmo-adaptation in *Saccharomyces cerevisiae*. *Science* **319,** 482–484 (2008).
16. Hersen, P., McClean, M. N., Mahadevan, L. & Ramanathan, S. Signal processing by the HOG MAP kinase pathway. *Proc. Natl Acad. Sci. USA* **105,** 7165–7170 (2008).
17. Pelet, S. *et al.* Transient activation of the HOG MAPK pathway regulates bimodal gene expression. *Science* **332,** 732–735 (2011).
18. Morgan, R. A., Dudley, M. E. & Rosenberg, S. A. Adoptive cell therapy: genetic modification to redirect effector cell specificity. *Cancer J.* **16,** 336–341 (2010).
19. June, C. H., Blazar, B. R. & Riley, J. L. Engineering lymphocyte subsets: tools, trials and tribulations. *Nature Rev. Immunol.* **9,** 704–716 (2009).
20. Morgan, R. A. *et al.* Case report of a serious adverse event following the administration of T cells transduced with a chimeric antigen receptor recognizing ERBB2. *Mol. Ther.* **18,** 843–851 (2010).
21. Brentjens, R., Yeh, R., Bernal, Y., Riviere, I. & Sadelain, M. Treatment of chronic lymphocytic leukemia with genetically targeted autologous T cells: case report of an unforeseen adverse event in a phase I clinical trial. *Mol. Ther.* **18,** 666–668 (2010).
22. Arbibe, L. *et al.* An injected bacterial effector targets chromatin access for transcription factor NF-κB to alter transcription of host genes involved in immune responses. *Nature Immunol.* **8,** 47–56 (2007).
23. Gerke, C., Falkow, S. & Chien, Y. H. The adaptor molecules LAT and SLP-76 are specifically targeted by *Yersinia* to inhibit T cell activation. *J. Exp. Med.* **201,** 361–371 (2005).
24. Lin, J. & Weiss, A. The tyrosine phosphatase CD148 is excluded from the immunologic synapse and down-regulates prolonged T cell signaling. *J. Cell Biol.* **162,** 673–682 (2003).
25. Yao, T., Mecsas, J., Healy, J. I., Falkow, S. & Chien, Y. Suppression of T and B lymphocyte activation by a *Yersinia pseudotuberculosis* virulence factor, yopH. *J. Exp. Med.* **190,** 1343–1350 (1999).
26. Kieback, E., Charo, J., Sommermeyer, D., Blankenstein, T. & Uckert, W. A safeguard eliminates T cell receptor gene-modified autoreactive T cells after adoptive transfer. *Proc. Natl Acad. Sci. USA* **105,** 623–628 (2008).
27. de Witte, M. A. *et al.* An inducible caspase 9 safety switch can halt cell therapy-induced autoimmune disease. *J. Immunol.* **180,** 6365–6373 (2008).
28. Bonini, C. *et al.* The suicide gene therapy challenge: how to improve a successful gene therapy approach. *Mol. Ther.* **15,** 1248–1252 (2007).
29. Ciceri, F. *et al.* Infusion of suicide-gene-engineered donor lymphocytes after family haploidentical haemopoietic stem-cell transplantation for leukaemia (the TK007 trial): a non-randomised phase I–II study. *Lancet Oncol.* **10,** 489–500 (2009).
30. Brandman, O. *et al.* Feedback loops shape cellular signals in space and time. *Science* **322,** 390–395 (2008).

Supplementary Information is linked to the online version of the paper at www.nature.com/nature.

Acknowledgements We thank K. Orth for the YopH plasmid; K. McNally and S. Neou for tissue culture support; H. El-Samad, C. Voigt, C. Tang and the Lim laboratory for discussions. We acknowledge the 2007 UCSF iGEM team (M. Chen, E. Chou, J. Huang, L. Jann, E. Meltzer, A. Ng and R. Ovadia) for their initial work on bacterial effectors in yeast. This work was supported by American Cancer Society fellowship PF-09-137-01-TBE (W.W.W), a Li Foundation Fellowship (P.W.), a California Institute for Regenerative Medicine fellowship (grant number TG2-01153) (J.S.P.), National Institutes of Health grants PN2EY016546, RO1GM055040, RO1GM062583 and P50GM081879 (W.A.L.), the NSF Synthetic Biology and Engineering Research Center (W.A.L.), the Packard Foundation (W.A.L.) and the Howard Hughes Medical Institute (A.W. and W.A.L.).

Author Contributions P.W., S.G.P. and W.A.L. initiated the project in yeast. W.W.W., E.E.C., A.W. and W.A.L. initiated the project in T cells. P.W., W.W.W. and W.A.L. wrote the paper. P.W. and S.G.P. planned and performed the experiments in yeast. W.W.W., P.W., E.E.C., J.J.O. and J.S.P. planned and performed the experiment in T cells.

Author Information Reprints and permissions information is available at www.nature.com/reprints. The authors declare no competing financial interests. Readers are welcome to comment on the online version of this article at www.nature.com/nature. Correspondence and requests for materials should be addressed to W.A.L. (lim@cmp.ucsf.edu).

METHODS

Yeast constructs and strains. All yeast constructs used in this study (Supplementary Table 1) were cloned using a combinatorial cloning strategy on the basis of the type II restriction enzyme AarI developed by Peisajovich *et al.*[31]. For the MAPK pathway specific inhibitory experiments, strains WP022 and WP116 were constructed from the W303-derived strain SP147 (Supplementary Table 2) by tagging the carboxy (C) terminus of endogenous Pbs2 or Ste5 with leucine zipper, respectively. To construct WP039 for measuring the nuclear Hog1 accumulation, the C terminus of endogenous Hog1 in wild-type W303 strain was tagged with GFP using standard integration technique. For the visualization of the nucleus, a histone protein Htb2 was C-terminally tagged with mCherry, expressed from the *ADH1* promoter, and integrated at *TRP1* locus. Endogenous Pbs2 was tagged with a leucine zipper by PCR integration and was used in synthetic feedback loops. Synthetic effector gene cassettes were integrated at the *LEU2* locus. Yeast promoters, terminator and the *PTP2* gene were PCR amplified from *Saccharomyces cerevisiae* genomic DNA (Invitrogen). YopH gene was a gift from K. Orth. The *OspF* gene was synthesized by Integrated DNA Technologies. All yeast genomic integrations were confirmed by yeast colony PCR.

Yeast flow cytometry experiments. Analysis of the pathway-dependent fluorescent protein (GFP and mCherry) expression in yeast cells was performed with the BD LSRII flow cytometer (BD Biosciences) equipped with a high-throughput sampler. For each experiment, triplicate cultures were grown in synthetic complete media to early log phase ($D_{600\,nm}$ = 0.1–0.2). At time = 0, 1.5 μM of α-factor (GenScript) or 0.4 M of KCl were added into parallel cultures to induce separately the mating- specific or osmo-specific pathway response. For mating response, 100 μl aliquots were taken at time = 0 and after 2 h of induction; for osmotic response, 100 μl aliquots were taken at time = 0 and after 1 h of induction. Each 100 μl sample aliquot was immediately mixed with 100 μl of cycloheximide (10 μg ml^{-1}) in 96-well plates to stop the protein synthesis. After incubating the samples at room temperature for 30 min in the dark to allow for the maturation of fluorescent proteins, the levels of fluorescence protein were determined by flow cytometry. For each read, 10,000 cells were counted, and the mean fluorescent density was calculated by Flowjo software (BD Biosciences) as the pathway output value, and the s.d. from triplicate experiments was indicated as the error bar.

Yeast microfluidics, fluorescent microscopy and image processing. Microfluidic yeast cell culture was performed in Y04C plates with an ONIX flow control system (Cellasic)[32]. Cultures were grown to mid-log phase ($D_{600\,nm}$ = 0.2–0.8) in synthetic complete media. Cells were diluted to $D_{600\,nm}$ = 0.01 in 600 μl of fresh media and sonicated at a minimum set of 11% for 1 s using a Fisher Scientific model 500 sonicator with a 2 mm tip. Cells were loaded into the flow chamber pre-coated with concanavalin A and flowed over by synthetic complete media for more than 20 min before applying the square pulse sequence. Pulse stimulation with salt media was performed by ONIX FG flow control software (Cellasic) with the flow pressure of 8 pounds per square inch. Image acquisition was performed with a TE2000-E automated inverted microscope (Nikon) with Perfect Focus and ×100 oil immersion lens.

Background subtraction was performed first on all fluorescence images using ImageJ (http://imagej.nih.gov). The subsequent image analysis for both nuclear Hog1–GFP import and *pSTL1*–mCherry expression was performed with custom MATLAB (Mathworks) software (developed by K.-Y. Lau from C. Tang's laboratory at University of California San Francisco). For Hog1–GFP import analysis, cell boundaries were first determined from the bright-field differential interference contrast microscopy images. Cell nuclei were segmented by mCherry-labelled nuclear images. The nuclear and total cell GFP densities were calculated from the GFP fluorescent images. For *pSTL1*–mCherry expression, cell boundaries were determined the same way Hog1–GFP localization and mCherry densities were determined from the mCherry fluorescent images. For all frequency responses, a 210 min time course of pulse stimulation was performed and the maximum value of each time course was taken as the output of the stimulation frequency. The population average of more than 50–100 cells was determined for each single measurement, each experiment was repeated at least three times (see also Supplementary Fig. 3c, d) and the s.d. was calculated with the three repeats.

***Jurkat* T-cell lines, plasmids and transfection.** The *Jurkat* T cell with *pNFAT*–EGFP (neomycin resistant) stably integrated into the chromosome is a Weiss laboratory stock strain. All plasmids were made by using standard cloning techniques, AarI combinatorial cloning technique[31] and Gateway cloning technique (Invitrogen). See Supplementary Tables for more cloning detail. *Jurkat* cells were maintained in RPMI 1640 supplemented with 10% heat-inactivated FBS (Invitrogen), extra L-glutamine (2 mM), penicillin, streptomycin and G418 (2 mg ml^{-1}, Invitrogen).

For transfection, *Jurkat* T cells were cultured in RPMI 1640 supplemented with 10% heat-inactivated fetal bovine serum (FBS) and glutamine (10G RPMI) for at least 1 day. Twenty million cells were spun down, washed once with 10G RPMI and re-suspended in 300 μl of 10G RPMI. Fifteen micrograms of each plasmid were added to each transfection, vortexed briefly and incubated at room temperature for 15 min. The cell/DNA mixture was then subject to electroporation (BioRad, square pulse, 300 V, 10 ms pulse, 0.4 cm cuvette). The cells were rested at room temperature for 10 min before re-suspending in 10 ml of 10G RPMI. The cells were allowed to recover overnight before performing further experiments. For transfection with plasmids that contained the *pTRE* promoter, the serum was switched to Tet-free serum (Clontech).

T-cell activation and doxycycline induction. TCR was activated with a *Jurkat*-specific anti-TCR antibody, C305 (ascites, University of California San Francisco antibody core) at 1:2,000 dilution unless stated otherwise at a cell density of 2.5 million cells per millilitre (for most experiments) or 0.5 million cells per millilitre (for doxycycline-inducible expression (100 nM) of effectors experiment). Phorbol 12-myristate 13-acetate (25 ng ml^{-1}) and ionomycin (1 μM) was also used to activate T cells in some experiment. For the dose–response curve, the highest dose of C305 was 1:600, serially diluted threefold to generate eight doses in total.

T-cell antibody staining and flow cytometry analysis. For staining of cell surface expression of CD69, cells were fixed and stained with anti-CD69-APC (BD). For staining of phosphorylated ERK, cells were fixed, made permeable by incubation with ice-cold 90% methanol on ice for 30 min and stained with primary antibody to phosphorylated ERK (4370 Cell Signaling) and anti-rabbit APC secondary antibody (711-136-152, Jackson Immunoresearch). All samples were analysed with a BD LSRII equipped with a high-throughput sampler. Live cells were determined from forward and side scattering. Transfected cells were determined by comparing cells without mCherry to cells transfected with *pEF*–mCherry. Only transfected and live cells were included in the analysis. Error bar represents the s.d. from three samples.

Western blot to determine protein expression level. One million live cells were quickly spun down and lysed on ice for 30 min. The supernatant was then spun down at 4 °C for 30 min. The lysates were then mixed with DTT and SDS sample loading buffer and boiled for 3 min. Samples were separated with SDS–polyacrylamide gel electrophoresis gel (4–12% Bis–Tris) and then transferred to nitrocellulose blot. The blot were stained with primary anti-HA antibody (Santa Cruz Biotechnology) and Li-Cor anti-mouse 680 LT secondary antibody. The blot was imaged with a Li-Cor Odyssey.

Human primary $CD4^+$ T-cell transduction. Human peripheral blood mononuclear cells were collected from normal donors and acquired as cell suspensions from flushed TRIMA leukoreduction chambers (Blood Centers of the Pacific). Primary $CD4^+$ T cells were purified by negative selection and Ficoll-Paque PLUS density medium separation (RosetteSep, Stem Cell Technologies). Purified cells were cryopreserved and placed in liquid nitrogen storage.

Replication-incompetent lentiviral particles were prepared in 293T cells by standard methods. Briefly, constructs of interest were cloned into the transfer vector pHR′SIN:CSW using standard molecular biology techniques and then co-transfected into 293T cells with the viral packaging plasmids pCMVdR8.91 and pMD2.G using the transfection reagent FuGENE HD (Roche). Amphotropic VSV-G pseudotyped lentiviral particles in the supernatant were collected 48 h later.

Before use, human primary $CD4^+$ T cells were thawed and cultured overnight in growth medium (X-VIVO 15 + 5% human AB serum + 10 mM N-acetylcysteine + 1× β-mercaptoethanol + 1× Primocin) supplemented with 30 U ml^{-1} IL-2. The next day, cells were activated with Dynabeads human T-Activator CD3/CD28 (Invitrogen) at a 3:1 beads-to-cells ratio. After 24 h of activation, the cells were transduced with lentiviral particles. In some cases, transduction was performed on RetroNectin-coated tissue culture plates to enhance viability and transduction efficiency. Briefly, non-tissue-culture-treated plates were coated with RetroNectin (32 μg ml^{-1}) and then blocked with PBS + 2% BSA. Viral supernatant was loaded into the wells and the plate was centrifuged at 1,200*g* for 1.5 h at room temperature. Finally, wells were washed once with PBS, activated T cells were loaded into the wells, and the plate was once again centrifuged at 1,200*g* for 1 h with reduced braking speed. T cells were then placed into the 37 °C incubator.

IL-2 release assay. Transduced cells were rested by culturing them for more than 10 days in the presence of 30 U ml^{-1} IL-2 added every other day for maintenance. Doxycycline (200 ng ml^{-1}) was added to the cells, which were then incubated for 6 h. Cells were washed and 5×10^4 human primary $CD4^+$ cells (transduced with the pause switch constructs or untransduced) were placed in a 96-well plate with 200 μl human growth media with activation agents added (10 ng ml^{-1} PMA + 0.5 μM ionomycin, magnetic Dynabeads coated with anti-CD3/anti-CD28 (beads:cells ratio, 0.3:1), or Raji B cells loaded with a superantigen cocktail). Doxycycline (200 ng ml^{-1}) was added into appropriate wells. After 24 h of incubation at 37 °C, the released IL-2 in the supernatant was measured with a human IL-2 ELISA kit II (BD Biosciences).

Human primary CD4$^+$ T-cell proliferation assay. Resting primary CD4$^+$ T cells were pre-treated with 200 ng ml^{-1} doxycycline for 6 h and then labelled with CellTrace Violet dye (Invitrogen). Fifty thousand dye-labelled human CD4$^+$ T cells were placed in a 96-well plate with 200 µl human growth media in the presence or absence of doxycycline (200 ng ml^{-1}) and Dynabeads coated with anti-CD3/anti-CD28 (beads:cells ratio, 0.3:1) to induce proliferation. After incubation at 37 °C for 4 days, the cells were assayed by flow cytometry. FlowJo curve fitting software was used to quantify cell proliferation as indicated by dilution of the CellTrace Violet dye in proliferating cells.

31. Peisajovich, S. G., Garbarino, J. E., Wei, P. & Lim, W. A. Rapid diversification of cell signaling phenotypes by modular domain recombination. *Science* **328,** 368–372 (2010).
32. Lee, P. J., Helman, N. C., Lim, W. A. & Hung, P. J. A microfluidic system for dynamic yeast cell imaging. *Biotechniques* **44,** 91–95 (2008).